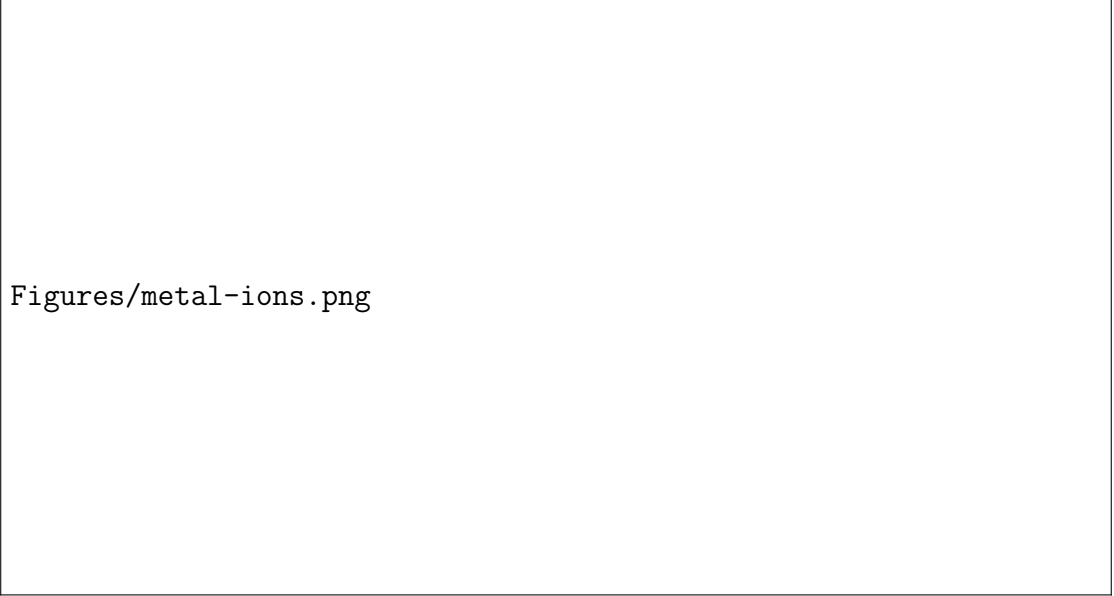# Contents

Chapter 1

Hunt for BLAs : The Survey

The foremost goal of the current study is to do a survey of BLAs over a large data-set and then estimate their contribution in the closure density of Ω_b. In this chapter we describe our approach to carry out this exhaustive survey.

1.1 Shortlisting the BLA candidates

Danforth et al. (2016) have identified a total of 2611 absorber systems in their study of the low redshift intergalactic medium. We need to find suitable candidates for our survey of BLAs from these 2611 absorbers.

We use two criterias to select BLA candidates for our survey. First, we look for broad Lyα lines in all the 2611 absorbers. For a Lyα line to be adjudged as 'broad', we fix our threshold for b value to be greater than 45 km s^{-1} in the preliminary fitting done by Danforth et al. (2016). Assuming a complete thermal broadening, $b = 45$ km s^{-1} gives a temperature of $\approx 1.2 \times 10^5$ K, which lies in the lower ranges of the temperature of WHIM. By giving this constrain, we get 568 such systems in the complete data-set.

As discussed in section **??**, multiple lines or contaminations from other lines can blend together to give rise to broad absorption features. In such cases, we need to carefully model these broad lines and confirm that these are actually tracing hot collisionally ionised gas phase so that they are indeed probing WHIM and

Figure 1.1 – No. of different metal ions in all the 29 absorber systems.

not just cool photoionised phase. We need to perform ionisation modelling for it. To model the ionisation conditions of the absorber systems, we need metal ion column densities. So we search for systems showing metal line absorption in these 568 'broad' systems. We need at least three distinct metal ions (not lines) to better constrain the ionisation state of an absorber system. This sets our second criteria that there should be minimum of three metal ion absorption in the absorber systems. Upon putting this constrain, we get 29 systems having at least 3 distinct metal ions out of 568 already identified systems. Out of these 29 systems, we have already studied one of the absorber in chapter **??**. Table 1.1 lists the lines of sight, redshift of the absorber and the ions detected in the systems these 29 identified BLA candidate absorber systems. Figure 1.1 shows the distribution of different metal ions found in these 29 absorber systems.

1.2 Survey methodology

We have identified 28 additional BLA candidate systems for our survey. We need to do the Voigt profile fitting to the absorption lines identified in these sys-

S. no.	Sight line	z_{abs}	Metal ions
1	1ES 1553+113	0.187731	C III, O VI, N V
2	3C 263	0.063275	C IV, Si III, Si IV
3	3C 263	0.140754	C IV, Si III, O VI
4	3C 57	0.077493	C IV, Si IV, N V
5	H 1821+643	0.170062	Si III, O VI, N V
6	H 1821+643	0.224832	Si III, O VI, C III
7	HE 0056-3622	0.043318	C IV, Si III, N V
8	PMN J1103-2329	0.003975	C IV, Si III, Si IV, N V
9	PG 0003+158	0.386094	C III, O VI, O III, N V
10	PG 0003+158	0.347586	C II, C III, Si II, Si III, O VI
11	PG 0003+158	0.421880	O VI, O III, C III
12	PG 0832+251	0.017520	C IV, Si IV, C II*, O I, Si III, C II, Si II, Fe II, Al II, N V
13	PG 1116+215	0.138527	C IV, Si IV, N II, P II, Si III, Si II, C II, O VI, N V
14	PG 1121+422	0.192434	Si IV, C III, Si III, Si II, C II, O VI
15	PG 1216+069	0.006390	O I, Si II, C II
16	PG 1216+069	0.282195	Si III, O VI, C III
17	PG 1222+216	0.054491	C IV, Si III, Si IV
18	PG 1222+216	0.378600	Si III, O VI, O III, C III
19	PG 1259+593	0.046107	C IV, Si III, Si IV
20	PG 1424+240	0.146789	C IV, Si III, O VI, Si IV
21	PHL 1811	0.080837	C IV, Si IV, N II, O I, Fe II, Si II, C II
22	PKS 0405-123	0.167125	Si IV, N II, C III, O I, Si III, Si II, C II, O VI, N III, N V
23	PKS 0637-752	0.161068	Si III, O VI, N V
24	PKS 0637-752	0.417573	Si III, O VI, C III
25	PKS 1302-102	0.094864	Si III, Si II, C II
26	RX J0439.6-5311	0.005602	C IV, Si III, Si IV
27	SDSS J135712.61+170444	0.097767	C IV, Si IV, Si III, C II, O VI
28	SBS 1108+560	0.463201	C III, O I, Si III, Si II, C II, O VI, N III
29	UKS 0242-724	0.063775	Fe II, Si II, C II

TABLE 1.1 – Details of the 29 BLA candidate absorber system shortlisted for the survey.

tems. These will give us the column densities and Doppler parameters of the ions in the system and also their redshifts (velocities). We will further use these quantities to model the ionisation conditions in these absorber systems.

The distribution of these quantities can give valuable insights towards our understanding of the intergalactic medium and the baryon content within IGM. As discussed in chapter **??**, that O VI is good tracer of WHIM. O VI absorption is seen in 16 out of these remaining 16 absorbers. For the remaining 12 candidates, O VI is not a non-detection. The O VI 1032, 1038 lines fall out the coverage of the HST/COS FUV channel at redshifts below ~ 0.093854 and all these remaining 12 systems are at redshift below 0.093854. So O VI is not covered in these systems. However, for one system which is along the LOS of PKS1302-102 at $z_{abs} = 0.094864$, the O VI 1038 line was just falling just on the edge of the spectrum where both S/N and sensitivity both low. So, O VI absorption was not considered for this system.

We first model the ionisation conditions in the 16 O VI absorbers and see if we can explain the origin of O VI through photoionisation models using the similar method used for the absorber in chapter **??**. For, the remaining 12 non-O VI absorber, we model the ionisation conditions based on the ions detected in the systems to estimate the density and metallicity in these systems.

Then, we will use the results from this survey to estimate the baryon content in BLAs and their contribution to cosmic closure density, Ω_b, the details of which are described in the upcoming chapter.

The Voigt profile fitting and ionisation modelling results are given in appendix **??** after the references.

1.3   Survey statistics

In this section, we discuss the statistics and results of the survey from Voigt profile fitting and ionisation modelling of the 29 absorber systems.
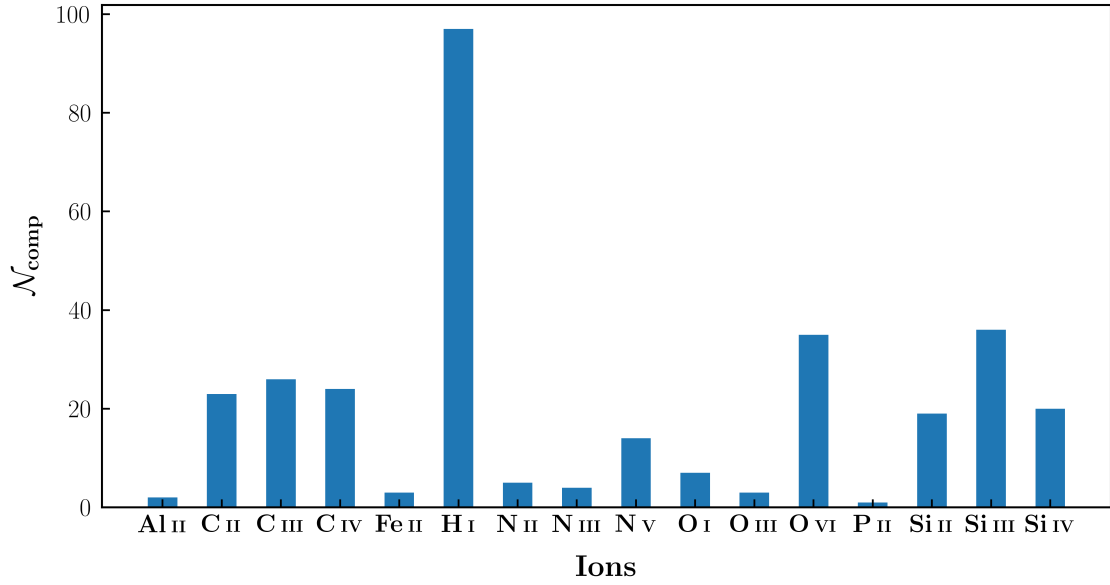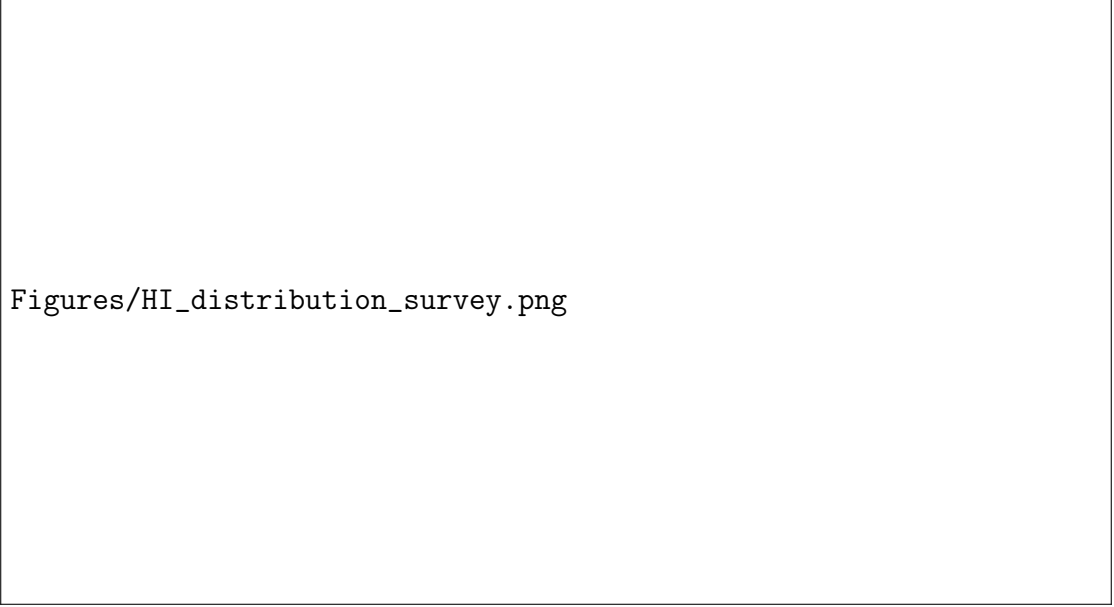
FIGURE 1.2 – No. of components identified for H I and different metal ions.

1.3.1 Voigt profile fitting

This survey of 29 absorbers spanned 22 lines of sight. These 22 lines of sight have total H I (Lyman-α) redshift pathlength of $\Delta z = 5.561$. A total of 413 absorption lines were identified and fitted with Voigt profiles. These 413 lines shown absorption from 15 different metal ions apart from H I absorption. The figure 1.2 shows the total number of components identified for each species. For studies similar to current one, it is very insightful to describe the line density per unit redshift ($d\mathcal{N}/dz$) and bivariate distribution of the absorbers with respect to column density and redshift ($\partial^2 \mathcal{N}/\partial N \, \partial z$) (see e.g. Danforth et al. (2016); Penton et al. (2000); Tilton et al. (2012)). However, since our current sample is not statistically large, we don't describe these metrics while discussing the statistics of the survey.

1.3.1.1 H I absorbers

We have identified 97 H I components in our survey across 29 absorbers. The figure 1.3 shows the distribution of column densities and redshift of these 97 components. These components span seven orders of magnitude of column densities
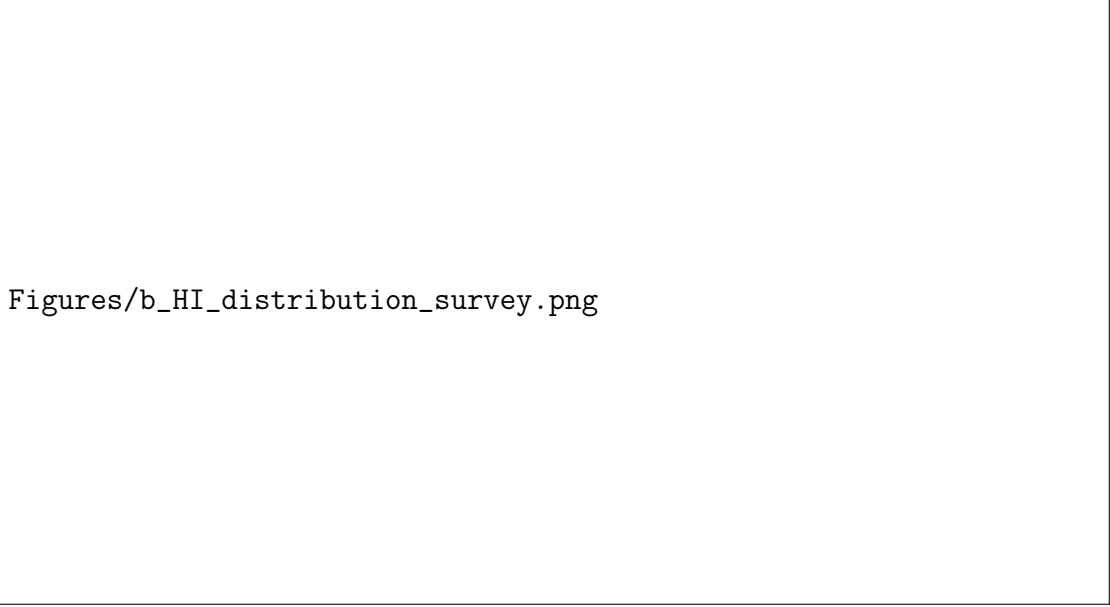
Figures/HI_distribution_survey.png

FIGURE 1.3 – Distribution of column densities (left panel) and redshift (right panel) of 97 H I components.

starting from $\sim 10^{13}$ to 10^{19} cm^{-2}. We have many absorbers with the column densities in the range $10^{13} - 10^{15.5}$ cm^{-2} but current sample is incomplete at rare large column density systems. In our current sample, we see H I absorption till $z \sim 0.45$. In redshift space also, we have more systems at lower redshifts ($z < 0.2$) and only few absorbers at higher redshifts.

Distribution of Doppler parameters

The figure 1.4 shows the distribution of Doppler b parameters of the 97 H I components. The vertical dashed line marks the cutoff for the line to be called as 'BLA' at b=40 km s^{-1}. Assuming a complete thermal broadening, $b = 40$ km s^{-1} gives a temperature of 10^5 K. Out of 97 components, 37(34) components have Doppler parameters in excess of 40(45) km s^{-1}. Some components show large Doppler widths of above 100 km s^{-1}, for this components only saturated Lyα lines are seen, making the identification of velocity substructures of these lines difficult. This results in the large b values for these lines.

Figures/b_HI_distribution_survey.png

FIGURE 1.4 – Distribution of b parameters of 97 H I components.

We can estimate the temperature of the gas directly from the Doppler parameter if we have Doppler parameter of another species coming from the same phase.
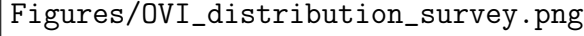
NH-bH plot

1.3.1.2 Metal absorbers

We have identified absorption from total of 15 distinct metal ions in our survey. In this section we discuss the statistics of some prominent ions in our sample.

O VI

We identified 35 O VI components in our survey across 17 absorber systems. O VI is the most common ion after Si III (36 components) in our sample, owing to the strong doublet lines at λ_{rest} = 1031.927, 1037.616 Å, with fairly large oscillator strengths of 0.1329 and 0.0661 respectively and large cosmic abundance of Oxygen. The figure 1.5 shows the distribution of column densities and redshifts of these 35 components. The O VI coverage starts from $z \sim 0.09$ in the HST/COS
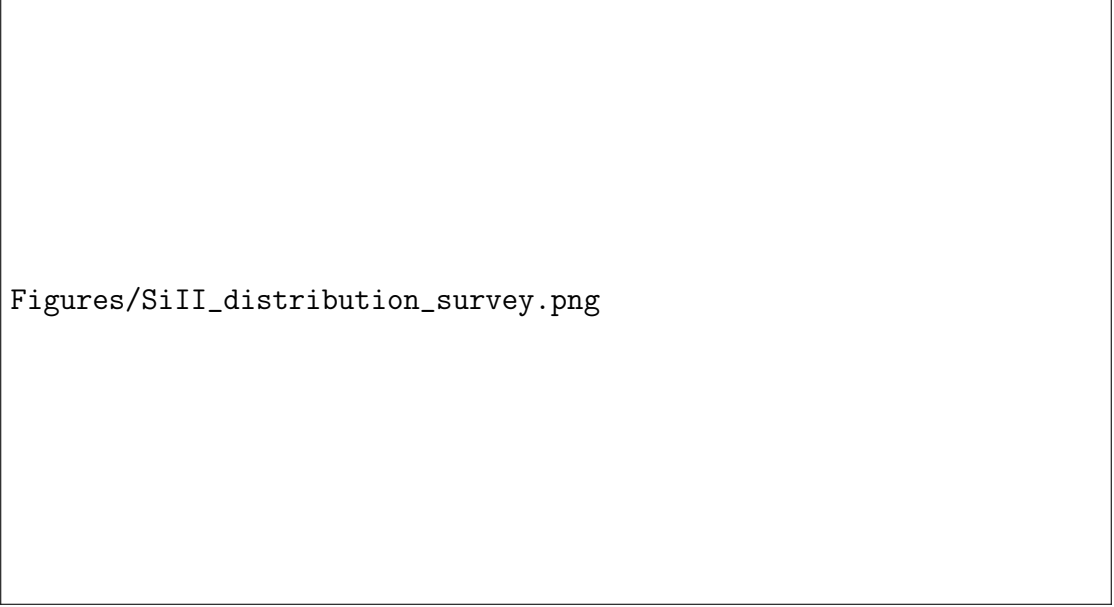
Figure 1.5 – Distribution of column densities (left panel) and redshift (right panel) of 35 O vi components.

FUV G130M grating. Unlike H i, we find O vi columnd densities in narrow range of $\sim 10^{13} - 10^{14.5}$ cm^{-2}.

O vi is a good tracer of WHIM at temperatures in range of $10^5 - 10^6$ K as its ionisation fraction peaks at around $10^{5.7}$ K in collisional ionisation (Gnat & Sternberg 2007). So, many studies of O vi absorbers have been done in detail in the past. Savage et al. (2014) have studied 14 QSO sight lines comprising a total of 56 O vi absorbers showing 85 O vi components. They estimate the baryonic content in warm gas traced by O vi as $\Omega_b(\text{O vi})_{\text{Warm}} = (0.0019 \pm 0.0005)h_{70}^{-1}$.

Studies exploring the correlations between star formation and O vi have also been done. In their study, Tumlinson et al. (2011, 2013) found strong correlation between the specific star formation rate and the presence of O vi. They found that star-forming galaxies are surrounded by large halos ionised O vi of sizes sim150 kpc, which were not much prominent around galaxies with little to no star-formation.

Figure 1.6 – Distribution of column densities (left panel) and redshift (right panel) of 19 Si II components.

Si II, Si III and Si IV

We find good number of Si absorbers in the form of Si II, Si III and Si IV ions having 19, 36 and 20 components respectively. Si II shows a number of lines in the COS/FUV channel with $\lambda_{\mathrm{rest}} = 1526.707, 1304.371, 1260.422$ Å and doublet at 1190.416, 1193.289 Å. Si III has the most components among the metal ions in our sample because of very high oscillator strength of 1.669 at $\lambda_{\mathrm{rest}} = 1206.5$ Å. And Si IV shows doublet line at $\lambda_{\mathrm{rest}} = 1393.760, 1402.772$ Å. Figures 1.6, 1.7 and 1.8 shows the distribution of column densities and redshifts of Si II, Si III and Si IV respectively.
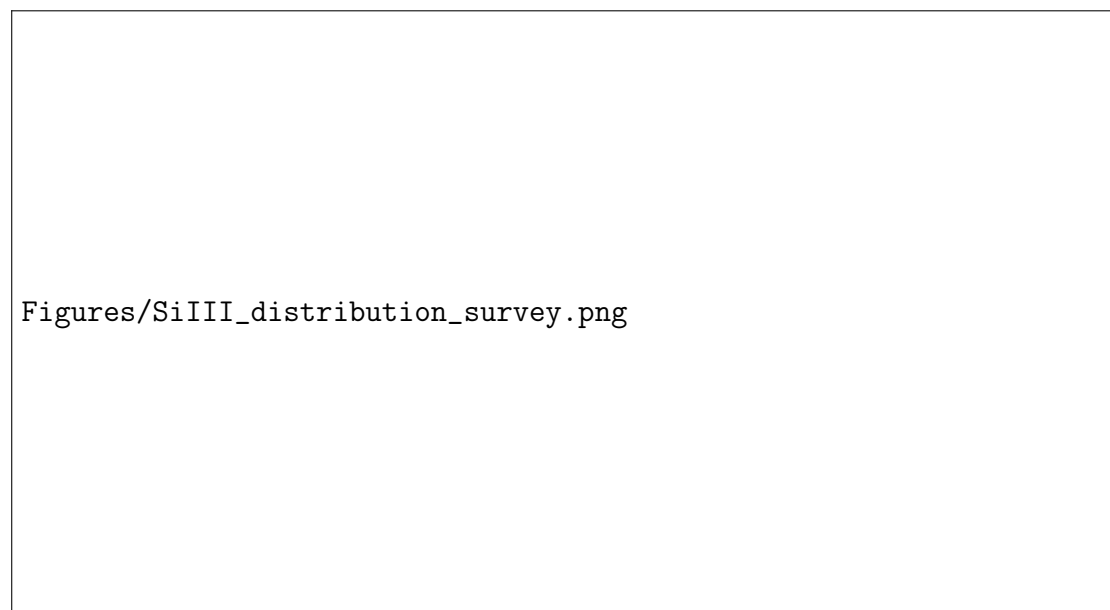
Figures/SiIII_distribution_survey.png

FIGURE 1.7 – Distribution of column densities (left panel) and redshift (right panel) of 36 Si III components.
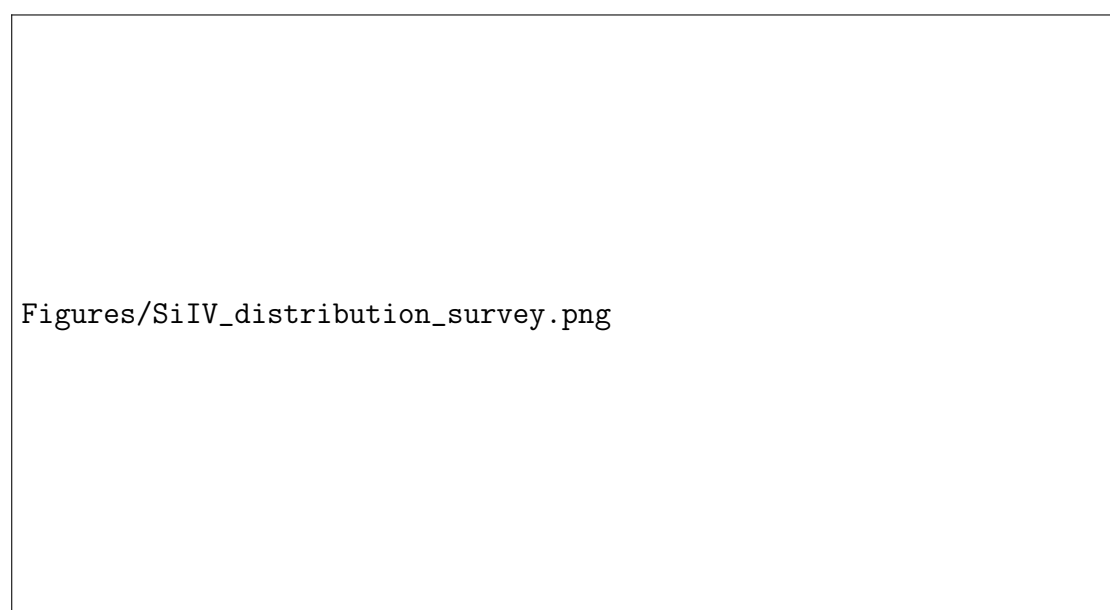
Figures/SiIV_distribution_survey.png

FIGURE 1.8 – Distribution of column densities (left panel) and redshift (right panel) of 20 Si IV components.

C II, C III and C IV

1.3.2 Ionisation modelling

1.4 Survey so far

Out of the 28 BLA candidate systems identified as described in section 1.1, we first focus on a subset of these systems which have O VI absorption, as O VI is a good tracer of WHIM. We have 16 such absorber systems. We begin the survey with these 16 systems. First step of the survey is to fit the Voigt profiles to all the lines identified in these systems. Currently, we have completed the preliminary fitting of these 16 absorber systems. The system plots of all these 16 systems are given in appendix **??**.

References

Danforth C. W., et al., 2016, The Astrophysical Journal, 817, 111

Gnat O., Sternberg A., 2007, The Astrophysical Journal Supplement Series, 168, 213

Penton S. V., Stocke J. T., Shull J. M., 2000, The Astrophysical Journal Supplement Series, 130, 121

Savage B. D., Kim T. S., Wakker B. P., Keeney B., Shull J. M., Stocke J. T., Green J. C., 2014, The Astrophysical Journal Supplement Series, 212, 8

Tilton E. M., Danforth C. W., Shull J. M., Ross T. L., 2012, The Astrophysical Journal, 759, 112

Tumlinson J., et al., 2011, Science, 334, 948

Tumlinson J., et al., 2013, The Astrophysical Journal, 777, 59